SUPPLEMENTARY INFORMATION FOR

Methylation of K9 in histone H3 directs alternative modes of highly dynamic interaction of heterochromatin protein hHP1β with the nucleosome

Francesca Munari[1,7], Szabolcs Soeroes[2,7,8], Hans Michael Zenn[3], Adrian Schomburg[2,8], Nils Kost[2], Sabrina Schröder[2,4], Rebecca Klingberg[5], Nasrollah Rezaei-Ghaleh[1], Alexandra Stützer[2], Kathy Ann Gelato[2], Peter Jomo Walla[4,6], Stefan Becker[1], Dirk Schwarzer[5], Bastian Zimmermann[3], Wolfgang Fischle[2], Markus Zweckstetter[1,9]**

[1]*Department for NMR-based Structural Biology, Max Planck Institute for Biophysical Chemistry, Göttingen, Am Fassberg 11, 37077 Germany*
[2]*Laboratory of Chromatin Biochemistry, Max Planck Institute for Biophysical Chemistry, Göttingen, Am Fassberg 11, 37077, Germany*
[3]*Biaffin GmbH & Co KG, Heinrich-Plett Strasse 40, 34132 Kassel, Germany*
[4]*Biomolecular Spectroscopy and Single-Molecule Detection, Max Planck Institute for Biophysical Chemistry, Göttingen, Am Fassberg 11, 37077 Germany*
[5]*Protein Chemistry, Leibniz-Institut für molekulare Pharmakologie, Robert-Rössle-Str. 10, 13125 Berlin, Germany*
[6]*Department for Biophysical Chemistry, Technische Universität Braunschweig, Hans-Sommerstr. 10, 38106 Braunschweig, Germany*
*Correspondence: wfischl@gwdg.de +49 551 201-1340; mzwecks@gwdg.de +49 551 201-2220
[7]These authors contributed equally to this work.
[8]Current Address: Oxford Nanopore Technologies LTD, Oxford, United Kingdom (SS); Proteros biostructures GmbH, Martinsried, Germany (AS)
[9]German Center for Neurodegenerative Diseases (DZNE), Göttingen, Germany

SUPPLEMENTARY METHODS

Protein expression constructs

Constructs for expression of *Xenopus laevis* core histones were kindly provided by Dr. Karoline Luger (Colorado State University). cDNA corresponding to human HP1β (GenBank NM_001127228), was PCR amplified using 5' primers that introduced a 6-HIS affinity sequence and a TEV cleavage site directly ahead of the translational start Met and cloned into the pET11a expression vector (Novagen). hHP1β sequences for NMR protein samples were cloned into pET16b expression vector: full-length (2-185), tail-less ΔNΔC (18-175), CD (19-79), CSD (107-176), and the monomeric mutant I161A. Site directed mutagenesis was carried out according to the Quickchange (Stratagene) protocol. Details of plasmid constructs are available upon request.

Expression and purification of recombinant hHP1β

Proteins were expressed in *E.coli* BL21 (DE3) RIL cells growing in ZYM-5052 auto-inducing medium. Proteins were purified on Ni-NTA beads (Qiagen) using standard protocols followed by anion exchange chromatography (MonoQ, GE Healthcare), and hydrophopic interaction chromatography (Phenyl-Sepharose, GE Healthcare). TEV protease cleavage was carried out at 1 mg/ml protein solution in TEV buffer (50 mM Tris-HCl, 50 mM NaCl, 1 mM DTT, 5% w/v glycerol, pH 8.0) using a molar ratio of 1 : 50 (TEV : protein) at 16˚C, over night. Free HIS-tag and HIS-tagged TEV protease were purified away by Ni-NTA chromatography. Purified recombinant proteins were dialyzed against 10 mM Triethanolamine-HCl, 150 mM NaCl, 1 mM DTT, pH 7.5 concentrated to >2 mg/ml using an Amicon Ultra centrifugal filter unit (Millipore), adjusted to 30% v/v glycerol, and stored at -20˚C.

Expression and purification of recombinant histones

Core histones were expressed and purified as described(1) with minor changes. ZYM-5052 auto-inducing medium was used instead of 2xYT for expression in *E.coli* BL21 (DE3) RIL cells. Also, after gel filtration chromatography on Sephacryl S 200 (GE Healthcare) peak fractions were pooled, diluted 5-fold into SAU0 (7 M deionized urea, 20 mM sodium acetate, 1 mM EDTA, 1 mM DTT, pH 5.2) and applied to a Q-Sepharose anion exchange column (GE Healthcare). The flow-through was subsequently applied to a SP-Sepharose cation exchange column (GE Healthcare), and eluted with SAU buffer using a linear NaCl gradient from 200 mM to 600 mM in 5 column volumes. Purified recombinant histone proteins were dialyzed extensively against H_2O or 2 mM dithiothreitol (in case of H3) at 4˚C, and lyophilized. Lyophilized proteins were stored at -80˚C.

Native chemical ligation

For recombinant H3 proteins carrying specific lysine 4 or lysine 9 mono-, di-, or trimethylation native chemical ligation was performed as described(2). Briefly, 0.2 mM of H3Δ1-20, A21C and 1 mM of the N-terminal H3 peptide (1-20) with a C-terminal thioester group were ligated for 24 hrs in 100 mM potassium phosphate, 3 M guanidine-HCl, 0.5% v/v benzyl mercaptan, 0.5% v/v thiophenol, pH 7.9 at 25˚C with vigorous mixing. The crude reaction mixture was dissolved into 25:75:0.1 acetonitrile:water:trifluoroacetic acid, diluted 5-fold into SAU-200 buffer (7 M deionized urea, 20 mM sodium acetate, 1 mM EDTA, 1 mM DTT, 200 mM NaCl, pH 5.2, applied to a Hi-Trap SP-Sepharose high performance cation exchange column (GE Healthcare), and eluted with a linear NaCl gradient from 200 to 600 mM. Protein samples were dialyzed extensively against 2 mM DTT at 4˚C, lyophilized and stored at -80˚C.

Site-specific installation of H3K$_C$9me3

H3K9C, C110A was expressed and purified as WT histones. Alkylation was performed as described(3). Briefly, 5 mM of mutant H3 was reduced for 1 hr at 37˚C in alkylation buffer (1 M HEPES, 4 M guanidium-HCl, 10 mM D/L-methionine, 20 mM DTT, pH 7.8). Alkylation reactions were performed at 50˚C in the presence of 400 mM (2-bromoethyl)-trimethylammonium bromide (Sigma) in the dark with occasional mixing. After 2.5 hrs of incubation, 10 mM of fresh DTT was added and the reaction was allowed to proceed for another 2.5 hrs at 50˚C. The alkylation reaction was quenched with 700 mM 2-mercaptoethanol, and the crude reaction mixture was diluted 50-fold into SAU-200 buffer. Purification of alkylated histones was as described above.

'Tail-transplantation' experiments

The H3 tail (residues 1-20) was fused to the very N-terminus of H2B (artificial Cys at -1 position) by native chemical ligation generating chimeric H2B-H3K9me3. As the H2B tail at 23 residues is significantly shorter than the H3 tail with 37 residues, this spaces the H3K9me3 modification in similar distance from the nucleosome core as in the wild type situation. To compensate for the 'transplantation' nucleosomes of H2B-H3K9me3 were reconstituted together with a truncated version of H3 (Δ1-20).

Reconstitution of histone octamers

Core histone octamers reconstitution was performed as described(1). Briefly, lyophilized purified WT core histones H2A, H4 and WT or modified H3 and H2B were dissolved in unfolding buffer and mixed to equimolar ratios. The histone mixture was extensively dialyzed at 4˚C against RB high buffer (10 mM Tris-HCl, 1 mM EDTA, 2 M NaCl, 1 mM DTT, pH 7.5) with at least three changes of dialysis buffer. Histone octamers were concentrated to 10-20 mg/ml using Amicon Ultra centrifugal filter units (Millipore) and purified on a HiLoad 16/60 Superdex 200 prep grade gel filtration column (GE Healthcare). Peak fractions were pooled and concentrated to at least 2 mg/ml. Histone octamers were stored in 50% v/v glycerol at -20˚C.

Reconstitution of recombinant mononucleosomes

The 187 bp DNA fragment used for nucleosome reconstitution was released from a plasmid containing 52 repeats of the 601 sequence with a 20 bp DNA linker on each side(4) after digestion with *BsoB*I (300 U/mg DNA). To separate vector backbone from the 187 bp fragment, DNA was

stepwise precipitated using PEG 6000/0.5 M NaCl (final PEG concentration 2-9% and 20%). DNA pellets were washed with 70% ethanol, dissolved in water and analyzed by gel electrophoresis. Fractions containing only the 187 bp DNA fragment were pooled.

Reconstitution of mononucleosomes was carried out as described(1). Briefly, stored octamers were dialyzed for at least 3 hrs against RB high buffer. Molar concentrations of octamers and DNA were determined photometrically according to the following equations: OD_{276} = mg/ml octamer (eq. 9.26 µM); OD_{260} = 50 µg/ml DNA (eq. 405 nM unlabeled or 390 nM biotinylated 187-601 DNA). For small-scale reconstitution of mononucleosomes, typically 0.1 µg/µl 187-601 DNA (eq. 0.8 µM) was mixed with histone octamers in a molar ratio of 0.8 to 1.2 octamers per DNA in 500 µl RB high buffer. The reaction mixture was dialyzed against RB high that was continuously replaced by RB low buffer (10 mM Tris-HCl, 1 mM EDTA, 10 mM NaCl, 1 mM DTT, pH 7.5) over a 36 hrs period using a peristaltic pump. Typically, a molar ratio of 0.9 octamers per 187-601 DNA resulted in saturated but not super-saturated mononucleosomes. For large-scale reconstitution of mononucleosomes 1 mg/ml 187-601 DNA (eq. 8 µM) was mixed with octamers in a molar ratio of 0.9 octamers per 187-601 DNA in RB high buffer. Nucleosome assembly was mainly performed as described above but over a 72 hrs period. Reconstituted mononucleosomes were extensively dialyzed against TEAE buffer (10 mM triethanolamine-HCl pH 7.5, 0.1 mM EDTA, pH 7.5) and stored at 4˚C.

NMR samples

BL21DE3 cultures for wild-type HP1β and its mutants were grown at 24°C and protein synthesis was induced overnight by addition of 0.4 mM IPTG at OD_{600}~ 0.6. For isotope labeling, minimal media containing $^{15}NH_4Cl$ and [^{1}H, ^{13}C]-glucose (double labeled) or $^{15}NH_4Cl$, [^{1}H, ^{13}C]-glucose in 99.9% $^{2}H_2O$ (fractional deuteration) or $^{15}NH_4Cl$, [^{2}H, ^{12}C]-glycerol in 99.9% $^{2}H_2O$ (perdeuteration) were used depending on the experimental requirements. For U-[^{2}H], Val, Leu-[$^{13}CH_3$, $^{12}CD_3$] samples, 100 mg l^{-1} of (3-methyl-^{13}C; 3,4,4,4-D4) α-ketoisovaleric acid (CIL) was added to the culture 1 hour prior to addition of IPTG(5) in the perdeuterared preparation. Protein purification was performed as described before. HP1β and nucleosome samples were dialyzed against 20 mM sodium phosphate (pH 6.5), 50 mM NaCl, 2 mM DTT and 0.02% NaN_3, prior to NMR measurements. Concentrations were adjusted with Vivaspin PES (Sartorius-Stedim biotech) centrifugal ultrafiltration devices depending on the experimental requirements.

Isothermal titration calorimetry

Mononucleosomes were reconstituted without scavenger DNA. Samples were concentrated to 200 to 300 µM using Amicon Ultra centrifugal filter units (Millipore) and dialyzed extensively against 10 mM triethanolamine-HCl (pH 7.5), 0.1 mM EDTA, 150 mM NaCl. Recombinant HP1β was concentrated to at least 2 mM and dialyzed against the same buffer. Lyophilized H3 peptides were directly dissolved in buffer.

Heats of dilution, obtained by titration of HP1β into buffer, were subtracted from raw data before analysis. Raw data were integrated, normalized, and the apparent heat change (Δq) of the reaction was plotted against the molecular ratio using the Origin® software. For determination of apparent enthalpy changes (ΔH_{app}), the molar association constant (K_A), and the stoichiometry (n) of the interaction, non-linear least-square fitting of the Δq values was performed by the Origin® software using a binding model of one set of identical binding sites. Thus, the heat change for each injection can be described by the equation

$$\Delta q_i = \frac{nc_{b,i}\Delta HV}{2}\left[1+\frac{c_{a,i}}{nc_{bi}}+\frac{1}{nK_A c_{b,i}}-\sqrt{\left(1+\frac{c_{a,i}}{nc_{bi}}+\frac{1}{nK_A c_{b,i}}\right)^2-\frac{4c_{a,i}}{nc_{b,i}}}\right]$$, where q_i is the molar heat

change, determined relative to zero for the unbound species (when saturation is reached), V the active cell volume, $c_{a,i}$ the total concentration of the injected component (e.g. HP1β) in the cell after the i^{th}

injection step, and $c_{b,i}$ the total concentration of the 'macromolecule' (e.g. H3 peptide or mononucleosomes) in the cell after the i^{th} injection step.

Surface plasmon resonance

Biotinylated ligands were immobilized on streptavidin coated sensor chips SA (GE Healthcare). Prior to immobilization, sensor chips were conditioned as described by the manufacturer. In order to obtain low surface densities (5-24 RU), 5 nM biotinylated H3 peptide was injected at a flow rate of 10 µl/min using varying contact times. High surface densities (> 700 RU) were prepared by injecting 3.5 µM peptide (10 µl/min) until the SA surface was saturated. Peptide containing chips were regenerated applying three short pules of 0.05% SDS followed by an injection of 1.5 M NaCl for baseline stabilization. Mononucleosomes assembled on 5'-biotinylated DNA were immobilized by injecting 1-2 µg/ml at varying contact times (10 µl/min) until the desired surface density was reached. Typically, ~240 and ~950 RU H3K9 modified mononucleosomes were coupled. In addition, unmodified mononucleosomes were immobilized on one SA surface (~950 RU). Regeneration of mononucleosome surfaces was conducted by applying a mixture of 0.1% Tween 20 and 0.1% NP40 diluted in running buffer (four consecutive injections for 30 seconds) and a subsequent injection of 0.5 M NaCl.

Qualitative and quantitative analyses of analyte binding to ligand were performed at a flow rate of 30 µl/min. A streptavidin surface without ligand served as reference. Additionally, blank runs were performed for double referencing. In order to determine apparent equilibrium dissociation constants (K_d), HP1β variants were injected in concentrations ranging from 24 nM to 50 µM (serial twofold dilutions) for two minutes. Dissociation was recorded for up to five minutes. Data evaluation was performed by steady state analysis assuming a Langmuir 1:1 binding model using the BIAevaluation software 4.1 and Prism 5.04 (GraphPad). Binding to the unmodified peptides and nucleosomes was analyzed with maximum binding (RU_{max}) set to the corresponding values obtained with the modified templates.

Analytical ultracentrifugation

Sedimentation velocity analysis was performed on an Optima XL-A analytical ultracentrifuge (Beckman-Coulter) using an An60Ti rotor and double sector cells (path length 12 mm). 400 µl samples at an OD_{260} of 0.3-1 in TEA buffer were analyzed at 20°C and a rotor speed of 35,000 rpm for mononucleosomes and 40,000 rpm for HP1β. The concentration profile was recorded by UV measurement at 260 nm. Buffer density, viscosity and protein partial specific volumes were calculated using the Sednterp software (http://www.rasmb.bbri.org/). Raw data was analyzed using the program Sedfit (version 11.8(6)). For each analysis 30 scans were continuously collected. The size distributions were calculated while floating meniscus, frictional coefficient and baseline, but keeping the buffer parameters constant, with a confidence level of $P = 0.68$, a resolution of $n = 150$, and sedimentation coefficients between 2 and 40 S.

SEC-MALLS measurements

Analysis was performed on a TSKgel G5000PWXL gel filtration column (Tosoh Bioscience) on a Postnova SEC system equipped with a Postnova PN 3070 MALLS detector using 10 mM Triethanolamine, 0.1mM EDTA, 150mM NaCl, pH 7.5. HP1β protein was extensively dialyzed into running buffer and injected in 20 µl at a concentration of 2 mg/ml at a constant flow rate of 0.5 ml/min. Interdetector delay was calculated by aligning the RI and MALLS-90°-signals using an ovalbumin monomer standard. Normalization was carried out with Pullulan 22. For RI and MALLS calibration, we used ovalbumin taking UV absorption into account.

Estimation of the ^{15}N cross-correlation rate (η_{xy}) if hHP1β would tumble together with the nucleosome core as a single rigid unit

In the fast exchange limit, the observed relaxation rates are population-weighted average of the rates of free and bound forms. At 1:2 HP1β/H3K_C9me3-nucleosome molar ratio, HP1β is partitioned between the free and bound states, the latter constituting ~54% of total HP1β, as estimated by NMR. The ^{15}N η_{xy} rates of the chromo domain in free HP1β are known through direct measurement. The η_{xy} rates of the bound form depend on the tumbling behavior of chromo domain in complex with nucleosome. Assuming that the chromo domain binds the core of the nucleosome particle and follows its tumbling behavior as a rigid body, the rotational correlation time (τ_c) of the nucleosome core can be used as a lower limit for τ_c of the bound chromo domain. This value was obtained through hydrodynamic calculations implemented in HYDROPRO(7), using the 3LZ1 nucleosome PDB file as input structure(8), where the flexible parts, i.e. histone and DNA tails, are not present. Taking the calculated τ_c (136 ns), η_{xy} values were derived through the following equation(9), assuming an axially symmetric ^{15}N chemical shift tensor, oriented with an angle θ between its unique axis and the N-H bond vector, and a rigid spherical molecule:

$$\eta_{xy} = \frac{\sqrt{3}}{6} c d P_2(\cos\theta)\{4J(0) + 3J(\omega_I)\},$$

where

$$d = -(\mu_0 \hbar \gamma_I \gamma_S) / (4\pi r^3_{IS})$$

and

$$c = \gamma_I(\sigma_{\parallel} - \sigma_{\perp})B_0 / \sqrt{3}$$

represent the spatial functions for dipolar coupling and chemical shift anisotropy relaxation mechanisms, respectively, with γ_H and γ_N as gyromagnetic ratios of ^1H and ^{15}N nuclei, $\mu_0=4\pi*10^{-7}$ as magnetic permeability of vacuum and $\hbar$ as the reduced Planck constant, r_{N-H} the ^{15}N-^1H internuclear distance, B_0 the magnetic field and ($\sigma_{\perp}$ - $\sigma_{\parallel}$) the difference of the two principal components of the axially symmetric ^{15}N chemical shift tensor. We used -173 ppm for ($\sigma_{\perp}$ - $\sigma_{\parallel}$) and 19.6 degree for θ, as recently suggested(10). J(ω), the spectral density function at frequency ω, was calculated at the two frequencies 0 and ω_N, using the τ_c as estimated by HYDROPRO and the isotropic rigid rotor diffusion approximation. The η_{xy} of the chromo domain in the bound state was then used together with the experimental η_{xy} value of unbound HP1β to predict the η_{xy} for the 46%/54% mixture of free and bound states. Note that the η_{xy} value obtained for chromo domain bound to the nucleosome core represents a lower limit since contribution of the chromo domain itself was not considered. Thus, the predicted η_{xy} value might be even higher, strengthening the hypothesis that HP1β remains highly flexible when bound to the methyl mark at histone H3 of a mononucleosome.

SUPPLEMENTARY REFERENCES

1. Luger, K., Rechsteiner, T. J., and Richmond, T. J. (1999) *Methods Mol Biol* **119**, 1-16
2. Shogren-Knaak, M. A., and Peterson, C. L. (2004) *Methods Enzymol* **375**, 62-76
3. Simon, M. D., Chu, F., Racki, L. R., de la Cruz, C. C., Burlingame, A. L., Panning, B., Narlikar, G. J., and Shokat, K. M. (2007) *Cell* **128**(5), 1003-1012
4. Robinson, P. J., Fairall, L., Huynh, V. A., and Rhodes, D. (2006) *Proc Natl Acad Sci U S A* **103**(17), 6506-6511
5. Tugarinov, V., Kanelis, V., and Kay, L. E. (2006) *Nat Protoc* **1**(2), 749-754
6. Schuck, P. (2004) *Biophys Chem* **108**(1-3), 187-200
7. Ortega, A., Amoros, D., and Garcia de la Torre, J. (2011) *Biophys J* **101**(4), 892-898
8. Vasudevan, D., Chua, E. Y., and Davey, C. A. (2010) *J Mol Biol* **403**(1), 1-10
9. Cavanagh, J., Fairbrother, W. J., Palmer, A. r., Rance, M., and N., S. (2007) *Protein NMR Spectroscopy: Principles and Practice, Second Edition*, ELSEVIER
10. Yao, L., Grishaev, A., Cornilescu, G., and Bax, A. (2010) *J Am Chem Soc* **132**(12), 4295-4309
11. Dam, J., Velikovsky, C. A., Mariuzza, R. A., Urbanke, C., and Schuck, P. (2005) *Biophys J* **89**(1), 619-634
12. Nielsen, P. R., Nietlispach, D., Mott, H. R., Callaghan, J., Bannister, A., Kouzarides, T., Murzin, A. G., Murzina, N. V., and Laue, E. D. (2002) *Nature* **416**(6876), 103-107
13. Kabsch, W., and Sander, C. (1983) *Biopolymers* **22**(12), 2577-2637

LEGENDS FOR SUPPLEMENTARY FIGURES

Supplementary Figure 1. Reconstitution of uniformly modified mononucleosomes and their interaction with HP1 proteins.
(A) ESI MS analysis of H3Δ1-20, A21C. (B) ESI MS analysis of H3K9me3, A21C. (C) The indicated proteins were run on SDS-PAGE and stained with Coomassie. (D) ESI MS analysis of H3K9C, C110A. (E) ESI MS analysis of H3K_C9me3, C110A. (F) The indicated proteins were run on SDS-PAGE and analyzed by Western blotting using the indicated antibodies (top) or Ponceau staining (bottom). (G) Schematic representation of the 187-601 DNA fragment used for mononucleosome reconstitution. The 601 nucleosome positioning sequence ('147-601', black), linker DNA ('L', grey), and the position of different restriction enzyme recognition sequences are indicated. (H) Mononucleosomes reconstituted at the indicated molar ratio of histone octamer:DNA fragments were analyzed by gel electrophoresis using 1% agarose buffered with 0.2 x TB. (I) Analysis of mononucleosomes using analytical ultracentrifugation. The C(s) method was applied to calculate the sedimentation coefficient distribution (c [s] as a function of S). The normalized distribution is shown as a red curve. By using the Bayesian assumption that only distinct species exist, the black curve is derived. (J-K) Analysis of histone octamer positioning on 187-601 DNA. Free 187x601 DNA and reconstituted mononucleosome (octamer:DNA, 0.9:1) were digested with the indicated restriction enzymes and analyzed by gel electrophoresis using a 2% agarose gel buffered with TBE. (L) Titration of hHP1β into H3K9me3-nucleosomes (0.12 μM) in TEA20 buffer analyzed by analytical ultracentrifugation. The sedimentation coefficient distribution C(s) is shown. The interaction of hHP1β with H3K9me3-mononucleosomes is fast and transient compared to the timescale of sedimentation otherwise a distinct species sedimenting at 14S would be observed(11). (M) ITC curves of injection of the recombinant hHP1β WT (600 μM) into H3K_C9me3-nucleosomes (20 μM). Top, raw data of heat release; bottom, integrated heats as calculated by the MicroCal Software. (N) Binding of hHP1β to the indicated mononucleosomes immobilized on sensory chips at high density (ca. 940 RU) was analyzed by SPR. Unscaled binding responses are plotted and fitted with a one-site binding model. Due to the very low binding to H3unmod nucleosomes, the saturation value (R_{max}) cannot be faithfully extrapolated. The dissociation constants (K_d) resulting from analysis under the assumption of correct extrapolation (R_{max} = 30) and under the assumption of saturation level equal to that observed for H3K9me3 (R_{max} = 113) are given in the table. Hill plot analyses of hHP1β binding to H3K9me3-mononucleosomes (O) and to H3K_C9me3-mononucleosomes (P) as measured by SPR. Data obtained at different immobilization levels (low, ca. 240 RU; high, ca. 940 RU) of nucleosomes are plotted. The resulting Hill coefficients are n_H(H3K9me3) = 0.82 and n_H(H3K_C9me3) = 0.89. (Q) Hill plot analysis of hHP1β binding to an H3K9me3 peptide as measured by fluorescence polarization. The resulting Hill coefficient is n_H(H3K9me3) = 0.83. (R) Scheme for the reconstitution and enrichment of asymmetrically H3K_C9me3-modified nucleosomes with only one of the two H3 tails carrying K9me3 and the other unmodified.

Supplementary Figure 2. Identification of the binding interface to H3K_C9me3-nucleosome by NMR spectroscopy.
(A) Selected regions from TROSY-[^{1}H, ^{15}N] HSQC spectra of hHP1β alone (blue), with H3K_C9me3-nucleosome at 1:2 molar ratio (red), with H3K_C9me3-peptide at 1:2 molar ratio (green) or unmodified nucleosome at 1:2 molar ratio (orange). (B) Chemical shift changes of hHP1β amide backbone resonances upon binding to H3K9me3-peptide (green) or H3K_C9me3-peptide (black) as a function of hHP1β residue number. In both cases the protein-peptide molar ratio is 1:2. Signals broadened beyond detection (V22, K43 and D62) or with severe signal overlap were excluded from the analysis. In the CSD slight nonspecific chemical shift changes were observed for residues 124-126 (see also with unmodified peptide in Supplementary Figure 5). (C) Correlation of ^{15}N-chemical shift differences (0.2ΔδN) between hHP1βΔNΔC (x-axis) and full-length hHP1β (y-axis) bound to the H3K9me3-peptide, relative to the free forms. In both cases, the ^{15}N values for bound-hHP1β were obtained from spectra recorded at saturation (1:2 protein-peptide molar ratio). (D) Correlation plot of relative

changes of ^{15}N and ^{1}H chemical shifts (i.e, $0.2\Delta\delta N/\Delta\delta H$) between hHP1β bound to H3K9me3-peptide (x-axis) and $H3K_C9me3$-nucleosome (y-axis) with respect to the free form. Only CD residues with chemical exchange that is fast on the NMR time scale were considered. (E)-(J) NMR cross-saturation transfer experiments. Spectra were recorded at 700 MHz using 0.1 mM U-[^{2}H, ^{15}N]-labeled hHP1β and unlabeled 0.01 mM $H3K_C9me3$-nucleosome. The intensity ratio of hHP1β signals recorded with (I_{sat}) and without (I_{ref}) selective saturation of nucleosome aliphatic protons is plotted versus the hHP1β sequence. A WURST-2 decoupling scheme centered at 0.9 ppm (E, F, G, H, I) and 2.9 ppm (J) was applied for 1.0 s before the TROSY-[^{1}H, ^{15}N] pulse sequence. Different temperatures were tested: 310 K (E), 303 K (F), 296 K (G), 289 K (H) and 282 K (I, J). Error bars were calculated on the basis of the signal-to-noise-ratios in the two spectra. Missing signals are due to severe signal overlap, or to broadening beyond detection at lower temperatures.

Supplementary Figure 3. Binding properties and characterization of the hHP1β I161A monomeric mutant.

In comparison with the WT hHP1β (A), the CSD in the monomeric hHP1βI161A (B) retained much more [^{1}H, ^{15}N] signal upon binding to the $H3K_C9me3$-nucleosome. The signal broadening was in between that observed for the isolated CSD (C) and the wild-type dimeric protein. The strong differences in signal broadening support the presence of hydrodynamic coupling of the CSD to the nucleosome. Spectra were acquired under identical experimental conditions using non-deuterated protein and 1:1 protein:ligand molar ratio. Top, schematic representation of the interaction measured. (D) Analysis of hHP1β WT (red) and mutant hHP1βI161A (black) by analytical ultracentrifugation. (E) SEC-MALLS analysis of hHP1β WT, UV absorbance trace (blue, left y-axis) and derived molecular mass (red dots, right y-axis) are blotted as a function of the elution volume. (F) [^{1}H, ^{15}N]-TROSY-HSQC spectra of the hHP1βI161A mutant (purple) and of hHP1β WT (green) proteins. Some residues of the chromo shadow domain, which are close to the site of mutation and experience large chemical shift changes, are labeled.

Supplementary Figure 4. Characterization of hHP1β/$H3K_C9me3$-nucleosome complex by methyl-TROSY NMR.

(A) [^{1}H, ^{13}C]-HMQC spectra of U-[^{2}H, ^{12}C], Val/Leu-[$^{13}CH_3$, $^{12}CD_3$]-labeled hHP1β alone (blue). (B) Superposition of the spectra of hHP1β free (blue), with $H3K_C9me3$-nucleosome (red), and with H3K9me3-peptide (green) both at a molar ratio of 1:2. The experiments were recorded at 310 K, at 800 MHz and in a 100% D_2O based buffer.

Supplementary Figure 5. Binding of hHP1β to the unmodified H3-tail peptide and the unmodified nucleosome.

(A) Selected regions of the [^{1}H, ^{15}N]-TROSY HSQC spectrum of free hHP1β (black) and of hHP1β with unmodified H3 tail peptide at 3:1 (green), 1:1 (yellow), 1:2 (light blue), 1:4 (blue) and 1:8 (red) molar ratio. (B) Chemical shifts changes of hHP1β ($\Delta\delta NH$) upon binding to unmodified H3 tail peptide (hHP1β/peptide molar ratio of 1:8) as a function of residue number. Despite the remarkable change in affinity, the perturbation profile is highly similar to that obtained with H3K9me3-peptide. The same set of peaks is involved and for most of the residues in the chromo domain the peaks shift along the same trajectory in the two titrations. Clear differences are only observed for residues (i.e W42, F45 and D49) that are in close proximity to the H3K9 N-methyl groups in the CD/methylated H3-peptide complex (PDB code: 1GUW(12)). (C) Superposition of [^{1}H, ^{13}C]-CT-HMQC spectra of U-[^{2}H, ^{15}N, ^{12}C], ^{13}C-Val-[$^{13}CH_3$,$^{13}CH_3$], ^{13}C-Leu-[$^{13}CH_3$,$^{13}CH_3$] labeled hHP1β alone (black) and with unmodified nucleosome (orange) at a molar ratio of 1:1. (D) [^{1}H, ^{13}C]-CT-HMQC spectra of hHP1β free (black) and with 601-DNA (red) at a molar ratio of 1:1. (E) [^{1}H, ^{13}C]-CT-HMQC spectra of hHP1β free (black), with unmodified H3 tail peptide at a 1:6 molar ratio (light blue), and with H3K9me3-peptide at a 1:1.5 molar ratio (green). The experiments in C, D and E were recorded at 303 K, 800 MHz in H_2O-based buffer. In this case constant time (CT) evolution was required as we used

the U-^{13}C5, 3-D1 α-ketoisovaleric acid precursor (CIL). (F) Primary sequence of hHP1β. Chromo and chromo shadow domains are highlighted in green and blue, respectively. Arrows and cylinders indicate β-strands and helices, respectively. Secondary structure elements were defined on the basis of the 3D structures (PDB codes: 1AP0 and 1DZ1) and by using the DSSP program(13). The star highlights the site of the I161A mutation that causes a disruption of the dimer interface. Y21, W42 and F45, which form the aromatic cage that specifically binds the tri-methylammonium moiety of H3K9me3, are shown in red.

SUPPLEMENTARY FIGURES

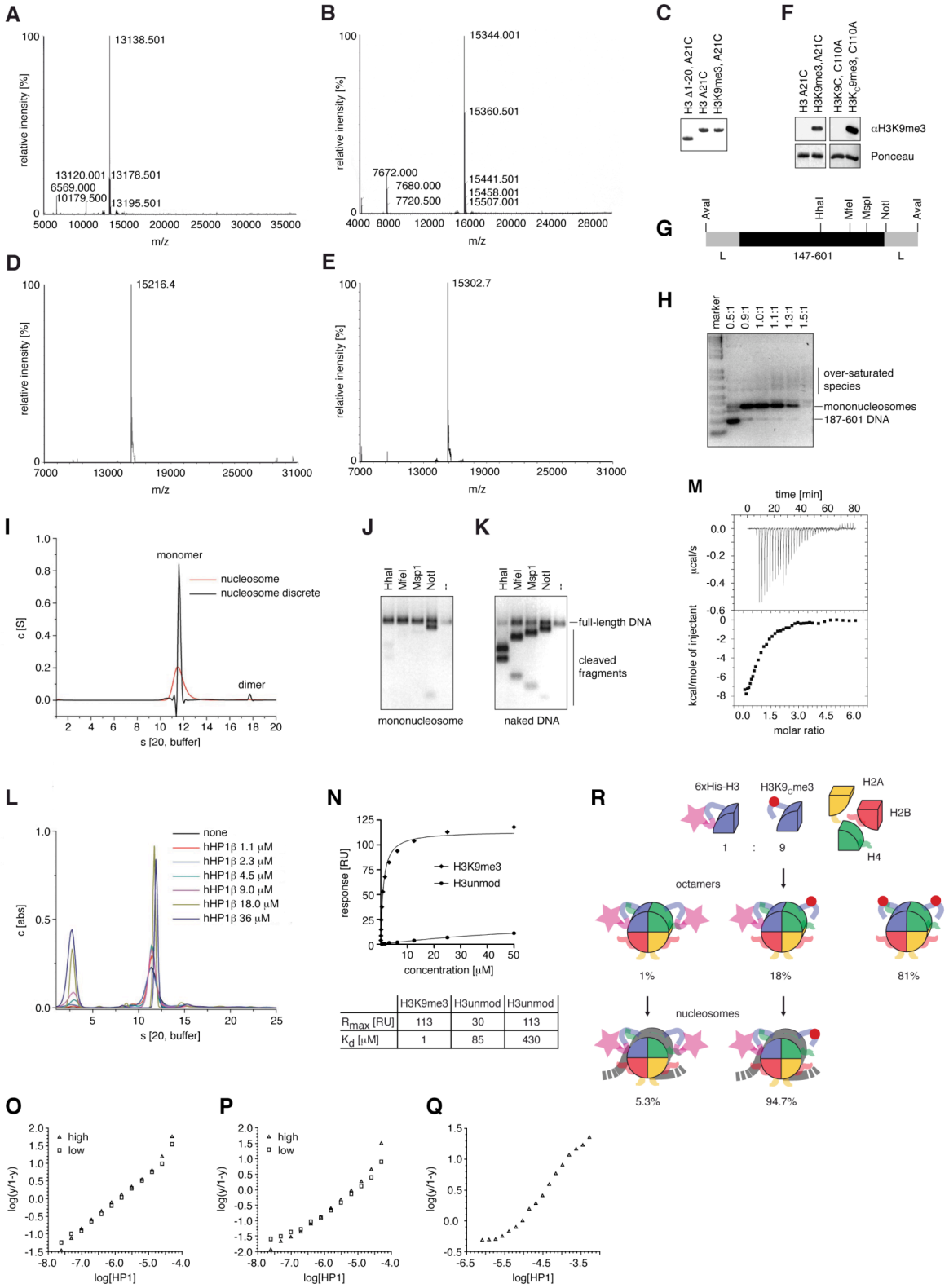

	H3K9me3	H3unmod	H3unmod
R_{max} [RU]	113	30	113
K_d [µM]	1	85	430

Supplementary Figure 1

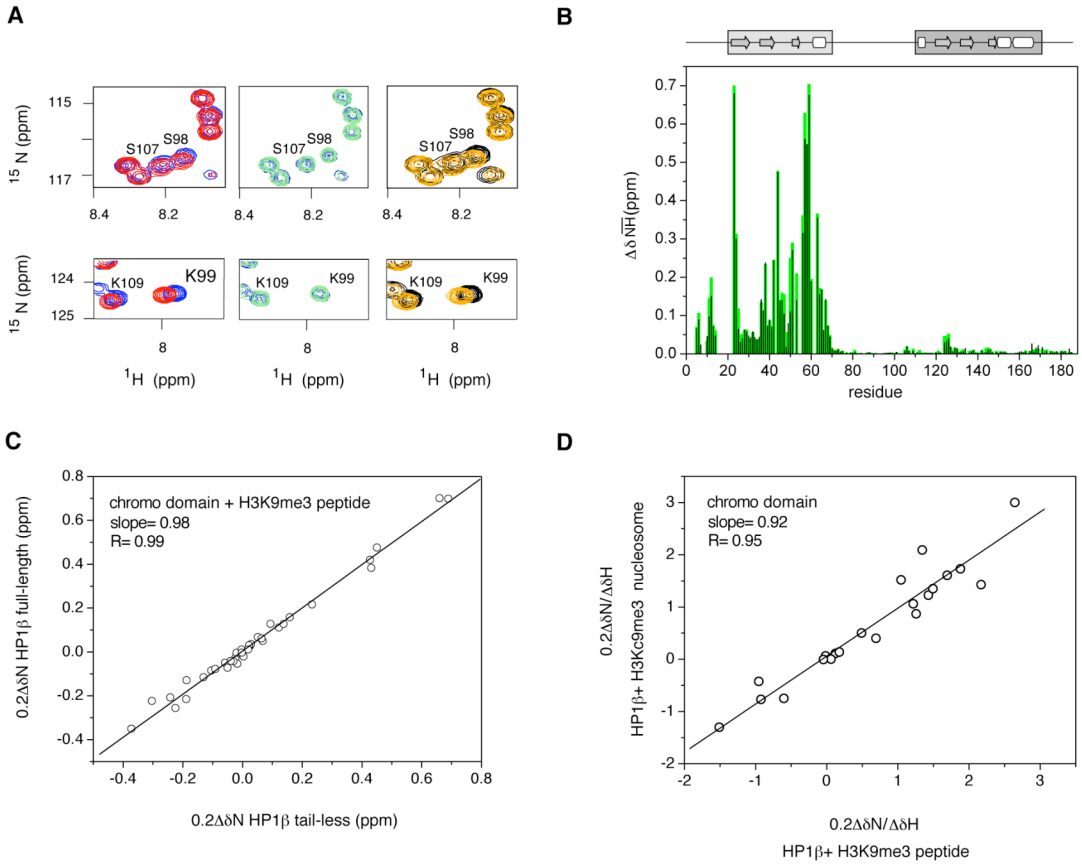

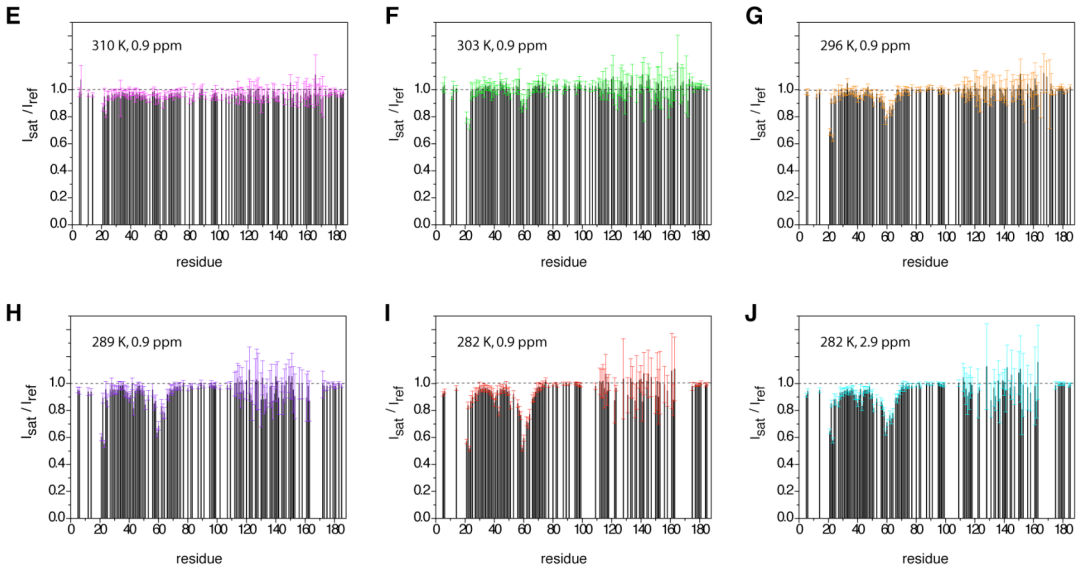

Supplementary Figure 2

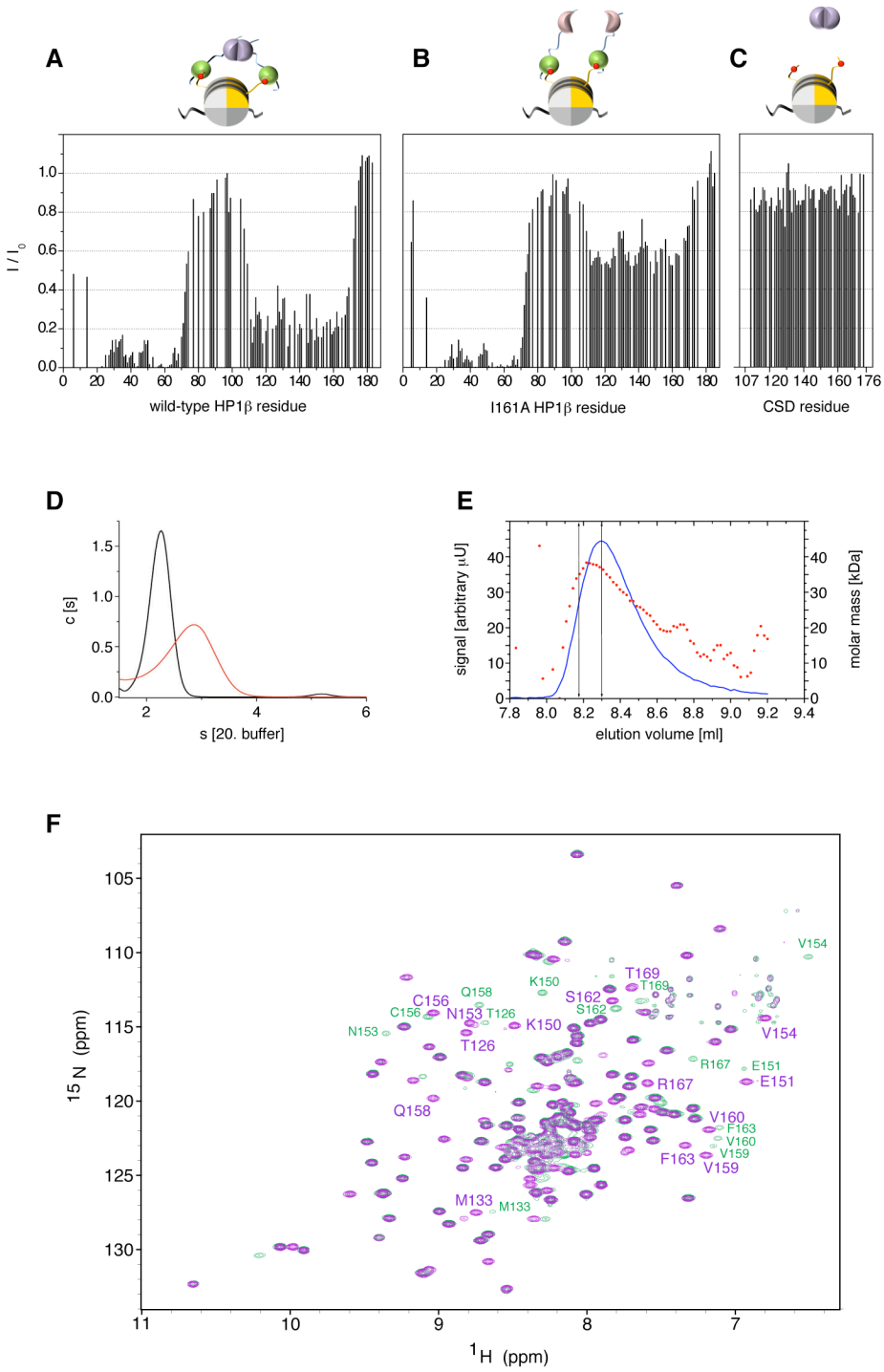

Supplementary Figure 3

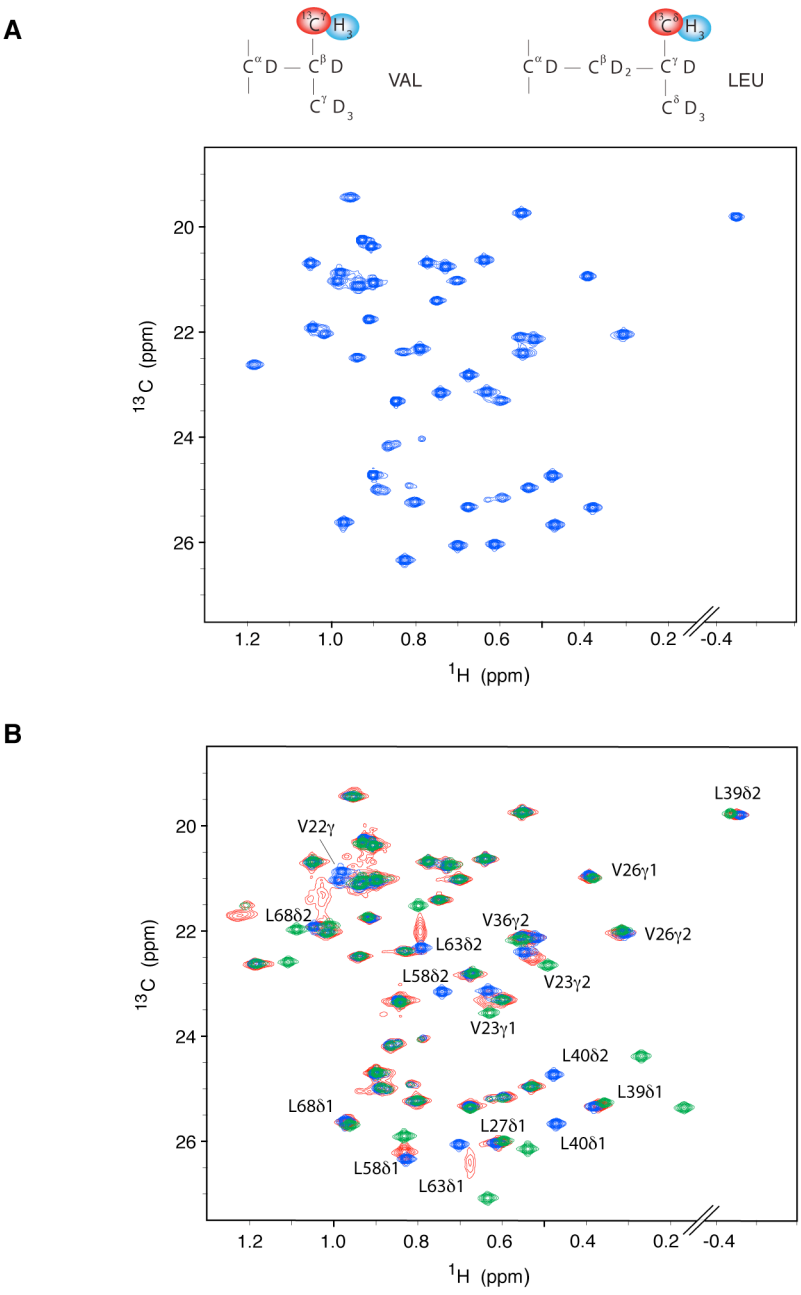

Supplementary Figure 4

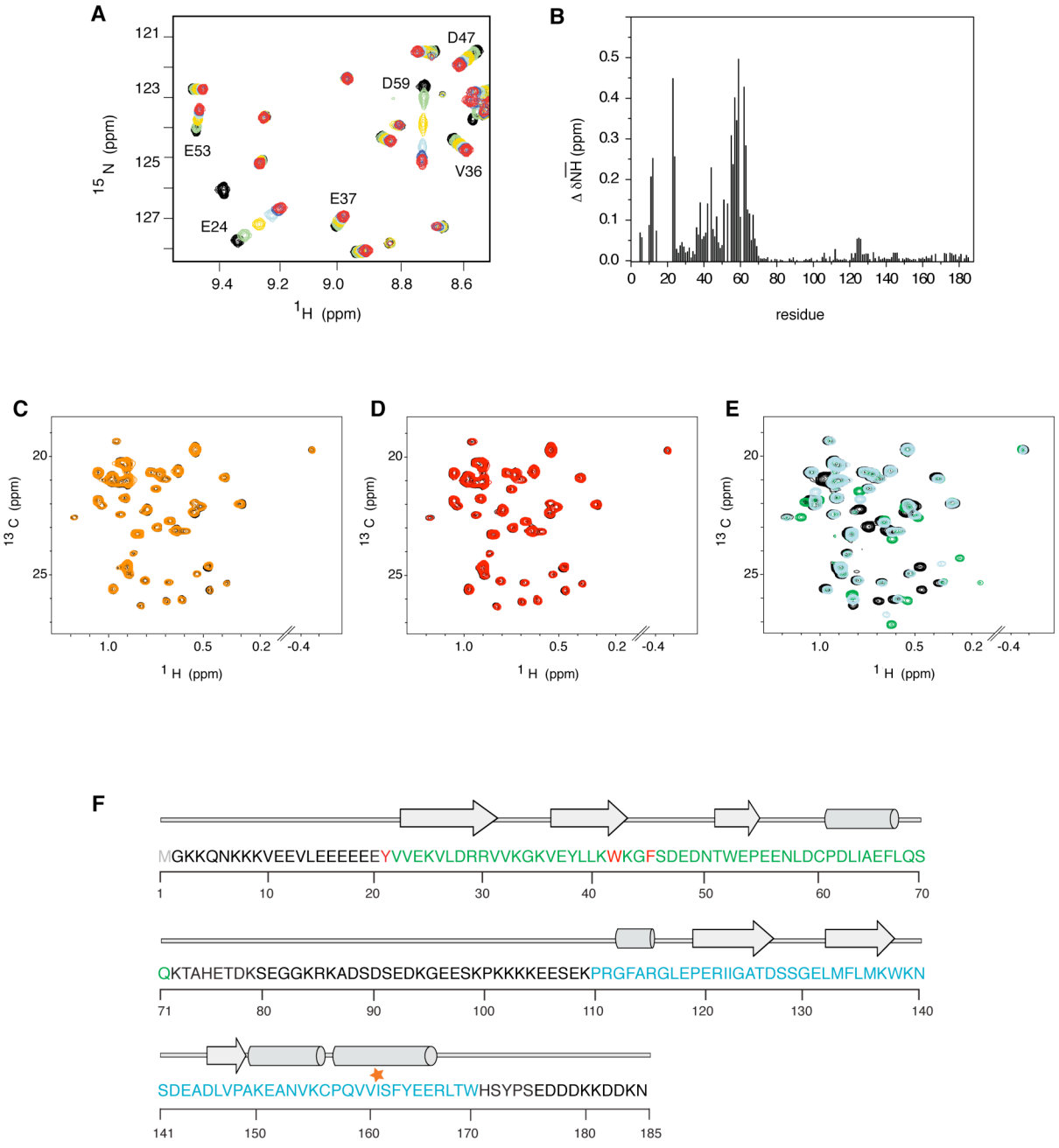

Supplementary Figure 5